Int. Conf. on Jets, Wakes and Separated Flows, ICJWSF-2010
Sept. 27–30, 2010, Cincinnati, Ohio USA

Experimental investigation on the effect of pulsations on turbulent flow through a 90 degrees pipe bend

Athanasia Kalpakli, Ramis Örlü, Nils Tillmark and P. Henrik Alfredsson

KTH CICERO, Department of Mechanics, Royal Institute of Technology, SE-100 44 Stockholm, Sweden

ramis@mech.kth.se

ABSTRACT

Pulsatile turbulent flows in curved pipes at high Dean numbers are prevalent in various components of internal combustion engines, particularly the intake of exhaust manifolds. Despite their technological importance, there is a clear lack of experimental data. The present paper provides preliminary, albeit unique, data from an experimental investigation, thereby addressing this gap and depicts impressions of the phase evolution of the complex flow including a back flow region. It is also shown, that due to the scale separation of the pulsations and the turbulence, the pulsatile flow can statistically be decomposed into its large-scale pulsations and the steady case.

1 INTRODUCTION

The gas flow in the exhaust system of an internal combustion engine (ICE) is quite complex due to several complications such as complex geometry, pulsating flow, compressibility, high temperatures, partly transonic conditions etc. Numerical simulations of such flow systems are generally favored, however these need to be validated against experiments in which the main physical features of interest are captured, in order to assess the accuracy and limitations of the simulations.

Besides the importance of gas flows in ICE, pulsatile flows in curved pipes are also present in e.g. respiratory flows and blood flows. This explains why most of the past studies reported in the literature are restricted to laminar [1] and incompressible [2] flows under low pulsation frequencies [3]. Although there are studies dealing with the flow in exhaust manifolds [4], these are mainly focused on straight pipes or the heat transfer in pipe bends [5]. Hence, there is a need for experimental data in pulsating turbulent flows in curved pipes at high Dean (De) and Womersley (α) numbers, defined by equations (1) and (2), respectively.

$$De = \sqrt{\gamma}\, Re, \tag{1}$$

$$\alpha = \frac{D}{2}\sqrt{\frac{\omega\rho}{\mu}}. \tag{2}$$

Hereby $Re = \rho U D/\mu$ and $\gamma = D/(2R_2)$ denote the Reynolds number and the curvature ratio, respectively, with R_2 being the bend centreline radius (see also figure 1).

In the present work the turbulent flow through a straight pipe and 90 degree pipe bend has been studied both under steady and pulsating conditions.

Mean and turbulence intensity profiles, probability density distributions, as well as phased-averaged statistics will be presented together with evolution snapshots from the mean flow development under a cycle. It will be shown, that despite the complexity of the flow under pulsating conditions in curved pipes, a simple scale decomposition of the pulsating flow can be performed to reveal the statistics of the steady case. This consequently suggests that the turbulence is merely superposed on the large-scale pulsating motion. Furthermore, back flow during the deceleration phase has been observed not only for the bend pipe, but also for the straight pipe section.

2 EXPERIMENTAL SET-UP

The experiments were performed at the Laboratory of KTH CICERO (*Centre for Internal Combustion Engine Research Opus*) in a newly developed flow rig that can be used both under steady and pulsating conditions. The set up, sketched in figure 1, consists of a long steel pipe (I) and a transparent Plexiglas (II) pipe section. The long pipe ends with either a straight pipe section (III) or a 90 degrees pipe bend (II). A rotating valve (V) in the pipe provides the pulsations and its frequency is controlled by means of a frequency regulated AC motor, which sets the rotation rate. The air is supplied through a compressor rig installation that can deliver up to 500 g/s at 6 bar. For details of the CICERO flow rig the reader is referred to Ref. [6].

Fluctuating mass flow rate density (ρu) measurements were performed with a hot-wire probe with a welded 5 micron tungsten wire of 1 mm length. The hot-wire was operated by means of a *DISA 55M01* main frame with a *55M10* standard CTA channel. The hot-wire was manually traversed across the horizontal and vertical axes, i.e. the y- and z-axes respectively, as indi-

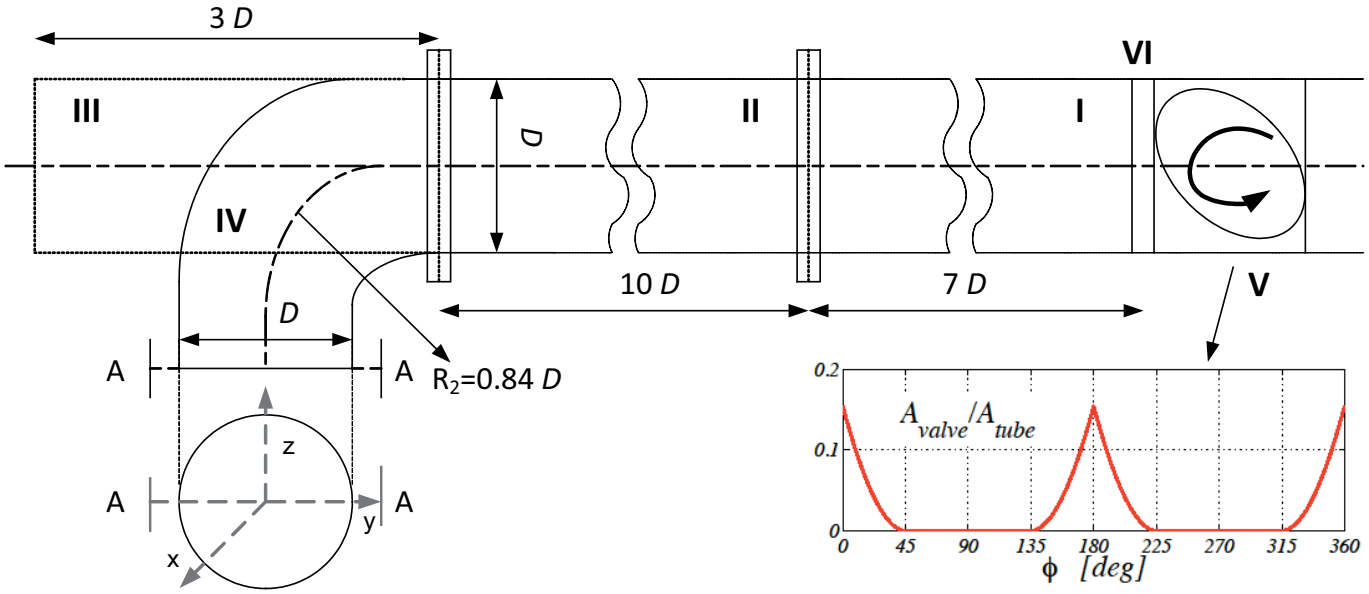

Figure 1: Schematic of the pipe bend configuration: I) Steel pipe section, II) Plexiglas pipe section, III) interchangeable straight brass pipe section, IV) interchangeable 90 degrees brass pipe bend, V) rotating valve, VI) smoke injection muff. The insert depicts the relative open area change caused by the rotating valve as function of revolution angle.

cated in figure 1. The mass flow was furthermore monitored by a hot-film type ABB mass flowmeter, that was mounted upstream the rotating valve. This was done to ensure steady inflow conditions to the flow rig as well as to provide a correct bulk mean mass flow rate for the non-dimensionalisation of the hot-wire readings.

Measurements were performed both under steady and pulsating conditions. The pipe has an inner diameter (D) of 39 mm, while the curved pipe section has a curvature ratio (γ) of 0.6. The results presented here were obtained at a mean mass flow rate of 120 g/s, corresponding to a Reynolds and Dean number of around 2×10^5 and 1.5×10^5, respectively. In the case of pulsating flow, a pulsation frequency of 40 Hz was chosen, giving a Womersley number of 80.

Although the flow under pulsating conditions is non-isothermal, the hot-wire readings presented here were not corrected for pulsatile temperature variations, due to missing instantaneous temperature measurements. Secondary flows in curved pipes are additionally present and falsify the hot-wire readings as well. However, based on the concept of effective velocity, the secondary components will not assert a too strong effect on the readings of a single hot-wire probe [7]. Hence the primary goal of the present investigation is not to provide an accurate quantitative assessment of the mass density rate, but rather to illuminate the qualitative effects of the pulsation and the curvature on the turbulent flow itself.

To ensure the correctness of the conclusions based on hot-wire measurements during the low speed phases, supplementary laser Doppler velocimetry (LDV) measurements have been performed for the straight pipe section at the pipe centreline. The LDV system is a single component *DANTEC FlowLite* system comprising a backscatter fibre optics probe, a 400 mm lens and a BSA F/P 60 processor. The source is a He-Ne laser of 10 mW emitting light with a wave length of 632.8 nm. The seeding particles were atomized oil (*Shell Ondina 27*) that was injected through an opening in a muff (VI) interconnecting the steel pipe section (I) and the pulse generator (V).

All measurements, both with the hot-wire and the LDV, were taken directly at the outlet of the straight pipe and the pipe bend, respectively.

3 RESULTS & DISCUSSION

3.1 General flow description

In figure 2 we show the mass flow rate measured by the hot-wire both in terms of the probability density distribution (pdf) as the colored band as well as the corresponding mean and rms-distributions (red and blue dots, respectively). Under steady conditions (left figure), despite the relatively short length of the straight pipe section between the pulse generator and the pipe outlet, the flow at the pipe outlet exhibits a well developed axi-symmetry, as evident from the mean and rms-distributions. Also the skewness and flatness distributions as well as profiles taken along the z-axis show axi-symmetry. Quantities with an asterisk in the superscript indicate non-dimensionalisation with the bulk mass flow rate density obtained from the ABB flowmeter. Furthermore the quantitative values agree well with what is known from fully developed turbulent pipe flow studies [8].

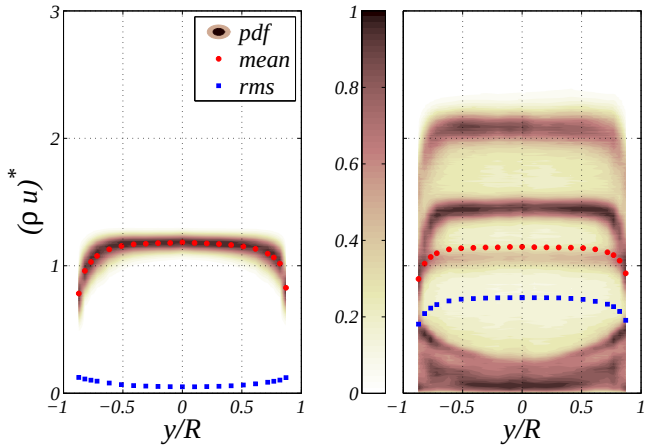

Figure 2: Contour plots of the probability density function of the mass flow rate density along the y-axis at the exit of the straight pipe together with its mean and root mean square value. *Left:* steady conditions, *right:* pulsating conditions (40 Hz).

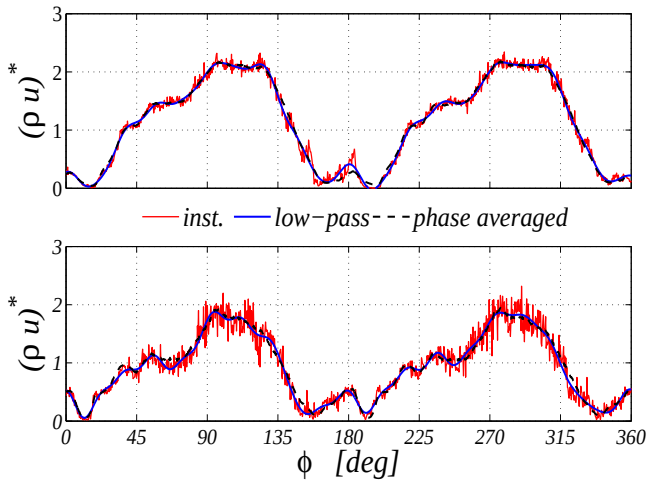

Figure 3: Instantaneous signal of the mass flow rate density at the exit of the straight pipe together with its low-pass filtered (f_c = 400 Hz) and phase-averaged ($\approx$ 200 valve cycles) counterpart. *Top:* $y/R = 0$, *bottom:* $y/R = 0.87$.

Under pulsating conditions the mean profile changes only slightly towards a more top-hat like profile, however the rms distribution exhibits quantitative and qualitative differences with respect to the steady counterpart. Here the rms is calculated on the full signal and is clearly dominated by the pulsating motion which is furthermore supported by the trimodal probability density function (pdf), which occurs due to the pulsatile motion. The time traces of the signal at two different radial positions are seen in figure 3. The trimodal behaviour of the pdf is apparent from the signals, there are three plateau-like regions, one just above zero (as will be discussed below this includes a region of back flow) and two at higher values.

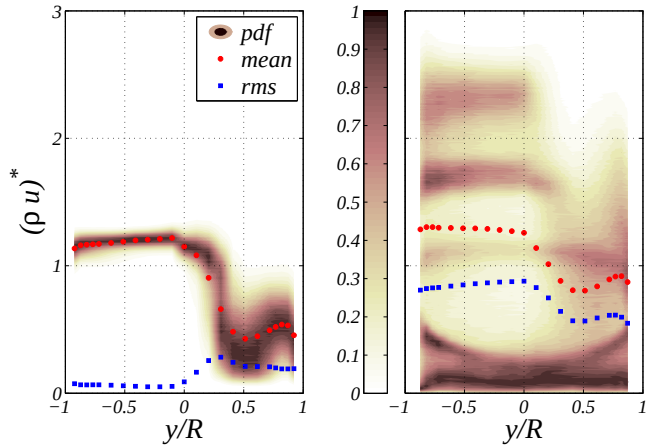

Figure 4: Contour plots of the probability density function of the mass flow rate density along the y-axis at the exit of the pipe bend together with its mean and root mean square value. *Left:* steady conditions, *right:* pulsating conditions (40 Hz).

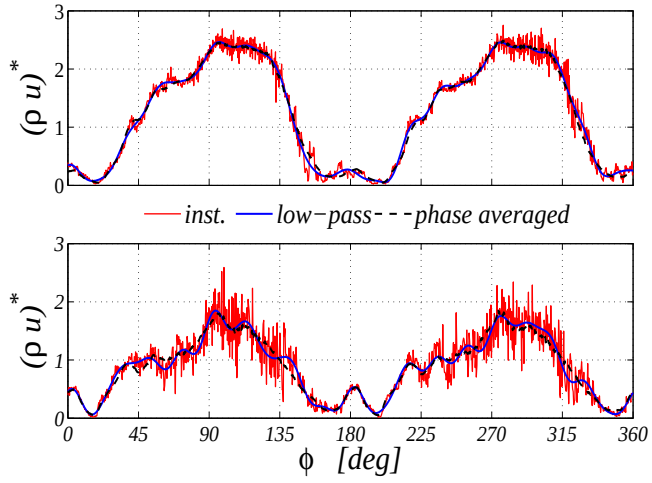

Figure 5: Instantaneous signal of the mass flow rate density at the exit of the pipe bend together with its low-pass filtered (f_c = 400 Hz) and phase-averaged ($\approx$ 200 valve cycles) counterpart. *Top:* $y/R = 0$, *bottom:* $y/R = 0.87$.

As can be seen both the latter have higher instantaneous flow rate than the mean value for the steady case. As expected the turbulence fluctuations, that seem to be merely superposed on the large scale pulsating motion, are higher closer to the wall as compared to the centreline, although this is not reflected in the rms-distribution.

In the case of the steady flow in the pipe bend, the mean profile, shown in the left part of figure 4, indicates that the fluid is strongly accelerated near the outer wall but also on the centreline the mass flow rate is higher, while simultaneously, it is decelerated near the inner wall, which is a result of an adverse pressure gradient generated by flow over a curved surface [9]. The pdf shows large fluctuations near the inner wall and the local

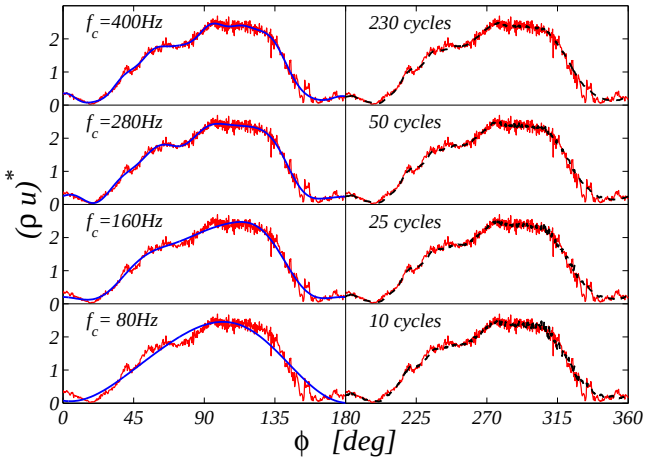

Figure 6: Same signal as in upper subplot of figure 3. Demonstration of the effect of different low-pass cut-off frequencies (shown in the region $0 \leq \phi \leq 180$) as well as the number of employed valve cycles for the phase averaging (shown in the region $180 \leq \phi \leq 360$).

turbulence level here is of the order of 50% or higher. Under pulsating conditions (right part of figure 4) the rms distribution resembles again very closely the one of the mean profile, similar to the steady case. In the outer part of the bend the pdf also resembles that of the straight pipe with three (or maybe even four) different plateaus.

Considering the pulsating flow cases, both in the straight pipe and pipe bend, it becomes evident that the pdf is particularly weighted towards the lower mass flow rate density side, and in particular it seems to have been squeezed towards zero. Recalling the inability of a hot-wire to sense the flow direction, the so called forward-reverse ambiguity [7], it seems plausible that instantaneous back flow is sensed as an equally strong velocity in the mean streamwise direction, i.e. x-direction. This can furthermore be observed when inspecting the instantaneous signals for the pulsating flow, as depicted in figures 3 and 5, for the straight pipe and pipe bend, respectively. While under steady conditions the instantaneous as well as low-pass filtered signals are unambiguously positive, the signals under pulsating conditions exhibit "reflections" at the abscissa, e.g. at around 160–200 and 340–20 degrees, which can be seen as an indication of back flow (cf. [7, 9]).

While the low-pass filtered and phase averaged signals for the straight pipe, shown in figure 3, demonstrate that both large-scale extraction techniques are equivalent, minor differences can be observed for the pipe bend, where the small-scale (high frequency) turbulence is more amplified compared to the straight pipe section. Here, the low-pass filtered representation of the instantaneous signal appears to be more representative than the phase averaged representation. Figure 6, on the other hand, demonstrates that phase averaging is a very robust method to extract the large-scale motion, while the low-pass filtered signal—as inherent in its definition—improves with increasing cut-off frequency, f_c. For the example shown in figure 6 the low-pass filtered signal approaches the phase averaged one at around 280 Hz and continues to improve further with increase in cut-off frequency. However, since the low-pass filtered signal for $f_c \to f_s/2$ approaches the instantaneous one, use of the low-pass filter requires pre-knowledge about the pulsatile motion (which albeit known here, is not always known in practise) in order to select a certain cut-off frequency. The phase averaging technique on the other hand appears to give a good and robust large-scale representation with as few as only 10 ensemble averages, in accordance with Ref. [9]. This also emphasises the excellent stability of the pulse generator.

3.2 Evidence of back flow

Back flow is a common phenomena in pulsating flows where the amplitude of the pulsations exceeds the bulk value, but even where this is not the case it can occur in curved pipes, due to secondary motions. As mentioned in the context of the pdfs shown in figure 2 and 4 and the instantaneous and phased-averaged signals depicted in figure 3 and 5, there are strong indications of back flow in both the straight and curved pipe. To further illuminate the presence of back flow ensemble averaged mean profiles have been computed for the deceleration

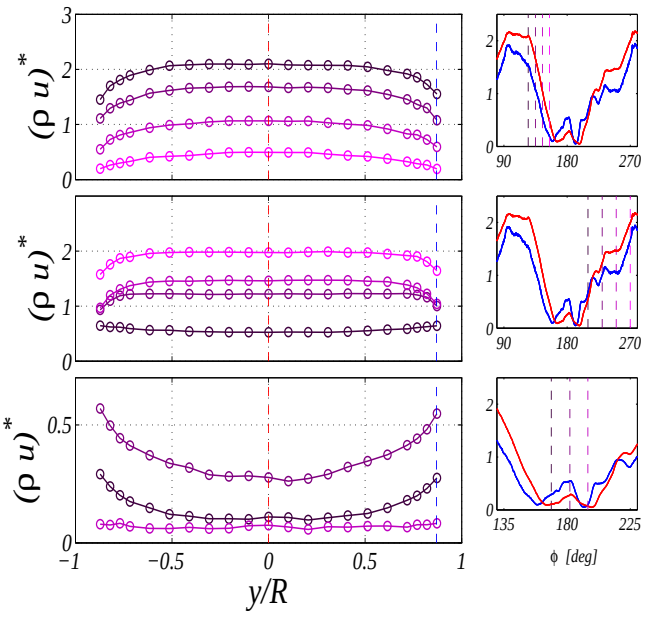

Figure 7: Ensemble averaged mean mass flow rate density profile along the y-axis for the straight pipe under pulsations for various phases. *Top:* deceleration phase, *middle:* acceleration phase, *bottom:* back flow region. Subplots on the right indicate the position in the phase averaged profile for $y/R = 0$ (red) and 0.87 (blue). Increasing phase positions are shown in progressively lighter shades of magenta. Note that the scale of the lower subplot is different.

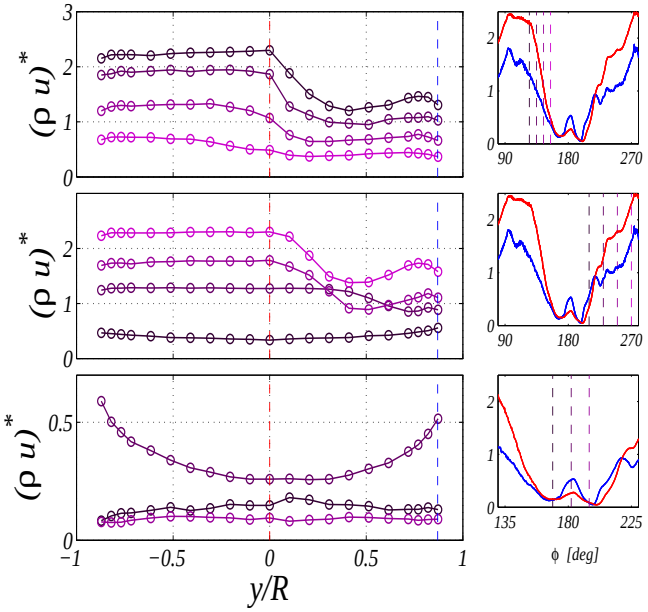

Figure 8: Ensemble averaged mean mass flow rate density profile along the y-axis for the pipe bend under pulsations for various phases. See caption of figure 7 for further details. Note that the scale of the lower subplot is different.

and acceleration phase as well as for the region in which back flow is suspected.

Figures 7 and 8 depict these ensemble averaged mean profiles for the straight and curved pipe, respectively. Considering the flow in the straight pipe, figure 7, it can be observed that the axi-symmetry is not only fulfilled in the long-time average, but throughout the pulsations. In particular for the deceleration and acceleration phase it becomes clear, that a flat turbulent pipe flow profile is present and appears to be carried on the large-scale pulsations. In accordance with Ref. [9], the profiles for the acceleration phase are flat over a large part of the central region. Flows starting from rest depict an even more profound top-hat profile [10] as evident from the middle subplots in figures 7 and 8 (see profile for $\phi \approx 200°$).

At the end of the deceleration phase the profiles approach the zero level and suspicion of back flow is supported by the inversion of the profile shape, i.e. the velocity around the centre of the pipe appears to be lower than closer to the wall. Similar observations can be made for the pipe bend, figure 8. However, here the strength of the back flow appears to be stronger.

The indication of back flow through the shown contour plots of the pdfs, figures 2–4, the phase-averaged signals, figures 3–6, as well as the ensemble averaged mean profiles, figures 7–8, was further substantiated by LDV measurements performed for the straight pipe under pulsating conditions to qualitatively confirm and quantitatively assess the presence of back flow. Due to the limitations of the optical arrangement of the present LDV settings velocity measurements were restricted to

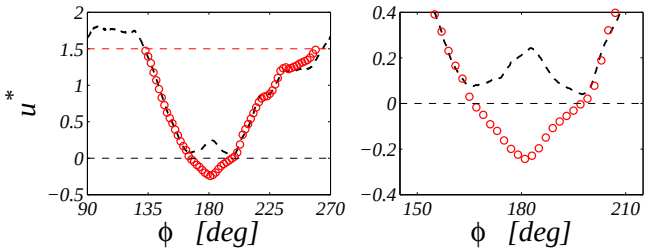

Figure 9: Comparison of phased-averaged mean streamwise velocity component at the exit at $y/R = 0$ for the straight pipe under pulsating conditions measured by means of hot-wire anemometry (dashed) and laser Doppler velocimetry (red circles). *Left:* Close-up of the deceleration and acceleration phase, *right:* close-up of the back flow region.

± 100 m/s. In order to cover the back flow region this range was set to -50 to 150 m/s and hence leaves out the high speed phases. Figure 9 therefore depicts a comparison between the phase-averaged mean streamwise velocity component measured by means of the hot-wire and the laser Doppler system. The close-up of the back flow region clearly indicates the fraction of back flow between 165 and 195 degrees, coinciding with the anticipated range from figures 3–6. It is also interesting to note that, despite the inability of the hot-wire to measure near zero velocity or to indicate the direction, it measures the correct amplitude of the back flow.

3.3 Decomposition into pulsatile and turbulent motions

Having concluded that the large-scale pulsatile motion is merely superposed on the small-scale "background" turbulence consequently leads to the statement that these scale separated motions can be considered independently from each other. In turn, it should be possible to decompose—to a high degree independent of the (reasonably) chosen cut-off frequency– -the pulsatile flow into two superposed scale-separated motions; one low-pass and one high-pass filtered signal, where the latter one gives very similar statistics to the one of the flow under steady conditions. To verify this, figure 10 depicts the rms distribution of both the steady and pulsed flow in the straight and the bend pipe. As anticipated the large-scale pulsatile motion is mainly responsible for the rms value of the pulsatile flow. Interestingly, the high-pass filtered signal (i.e. the "background" turbulence) is not only qualitatively, but also to some degree quantitatively identical to the rms distribution of the steady flow. It is also shown that the choice of the cut-off frequency is a rather insensitive parameter, which again supports the view of a linear superposition of two independent motions. It should, however, be kept in mind, that the turbulence time scale is around two orders of magnitude smaller than the pulsation period, and hence the con-

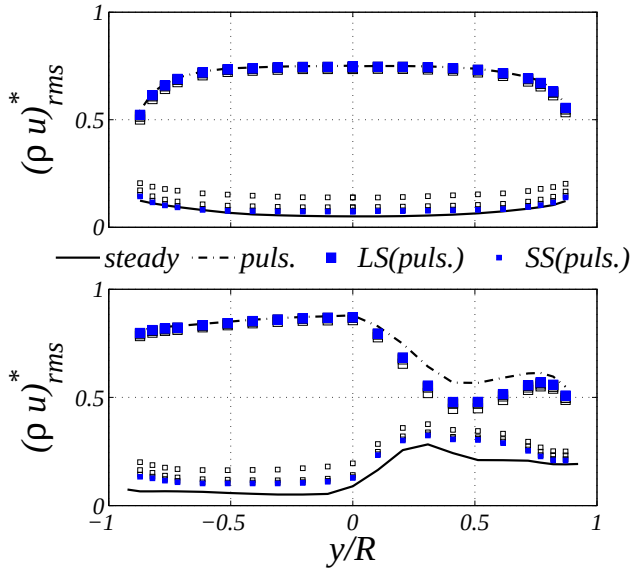

Figure 10: Root mean square distribution of the mass flow rate density along the y-axis for the steady (solid line) and pulsating (dash-dotted line) flow. Decomposition into a periodic large-scale (LS) and "background" small-scale (SS) contribution of the rms distribution by means of a filter with the cut-off frequencies employed in figure 6, viz. 80, 160, 280 (open symbols) and 400 (filled symbols) Hz. *Top:* straight pipe, *bottom:* pipe bend.

clusions drawn here should not be carried over to cases where the time scales are of the same order of magnitude. Nevertheless, the scale separation found here is comparable to those that can be found in intake pipes of exhaust manifolds and the conclusions drawn should therefore be relevant in this context.

4 SUMMARY & CONCLUSIONS

Hot-wire measurements of the mass flow rate density were performed in a newly developed flow rig for steady and pulsating flows. Mean and rms profiles, pdf distributions, time series, phase-averaged and low-pass filtered signals, as well as ensemble averaged phase evolution of the mean profiles have been presented for a straight pipe and a pipe bent at high Reynolds number. Due to the lack of studies for the parameter range covered here, these results provide unique, albeit preliminary, data in a parameter range related to the exhaust manifold of ICE.

Despite the complexity of the flow under pulsating conditions as well as in curved pipes, it has here been shown that a simple decomposition into a large-scale pulsating and a small-scale "background" turbulence is possible. In fact, the long-time statistics of the decomposed small-scale part of the pulsating flow resemble to a high degree qualitatively and quantitatively the statistics from the steady flow. This indicates, that the large-scale pulsating motion, due to the wide scale separation, is merely superposed on the turbulence.

Furthermore, a back flow region has been observed for the pulsatile flow, not only for the bend pipe section, but also for the straight pipe. In pulsatile flows the possibility of a non-negligible fraction of back flow should particularly be considered in light of its consequences for mass flow rate measurement techniques based on hot-wire/film anemometry, where the inability to detect the flow direction can lead to an overestimation of the mass flow rate. Nevertheless, it has also been demonstrated that hot-wire data can indicate back flow and even give its correct amplitude.

ACKNOWLEDGEMENT

This research was done within KTH CICERO, a centre supported by the Swedish Energy Agency, Swedish Vehicle Industry and KTH. The first author acknowledges the travel grant from the *Erik Petersohns* foundation.

References

[1] Sumida, M., *Pulsatile entrance flow in curved pipes: effect of various parameters*, Exp. Fluids, Vol. 43, pp. 949–958, 2007.

[2] Mullin, T., Greated, C.A., *Oscillatory flow in curved pipes. The fully developed case. Part 2*, J. Fluid Mech., Vol. 98, pp. 397–416, 1980.

[3] Sudo, K., Sumida, M., Yamane, R., *Secondary motion of fully developed oscillatory flow in a curved pipe*, J. Fluid Mech., Vol. 237, pp. 189–208, 1992.

[4] Capobianco, M., Gambarotta, A., Nocchi, M., *Unsteady Flow Phenomena and Volume Effects in Automotive Engines Manifolds*, SAE, 931897, 1993.

[5] Bauer, W.D., Wenisch, J., Heywood, B.J., *Averaged and time resolved heat transfer of steady and pulsating entry flow in intake manifold of a spark-ignition engine*, Int. J. Heat Fluid Flow, Vol. 19, pp. 1–9, 1998.

[6] Laurantzon, F., Tillmark, N., Alfredsson, P.H. *A pulsating flow rig for analyzing turbocharger performance*, 9th Int. Conf. on Turbocharging and Turbochargers (IMechE), pp. 363–372, 2010.

[7] Bruun, H.H., *Hot-wire anemometry. Principles and signal analysis.*, Oxford University Press, 1995.

[8] Schlichting, H., *Boundary-layer theory.*, McGraw-Hill Book Company, 7th ed., 1979.

[9] Chandran, K.B., Yearwood, T.L., *Experimental study of physiological pulsatile flow in a curved tube*, J. Fluid Mech., Vol. 111,pp. 59–85, 1981.

[10] Boiron, O., Deplano, V., Pelissier, R., *Experimental and numerical studies on the starting effect on the secondary flow in a bend*, J. Fluid Mech., Vol. 574, pp. 109–129, 2007.